Since January 2020 Elsevier has created a COVID-19 resource centre with free information in English and Mandarin on the novel coronavirus COVID-19. The COVID-19 resource centre is hosted on Elsevier Connect, the company's public news and information website.

Biosensors and Bioelectronics 193 (2021) 113535

Contents lists available at ScienceDirect

Biosensors and Bioelectronics

journal homepage: www.elsevier.com/locate/bios

One-pot pre-coated interface proximity extension assay for ultrasensitive co-detection of anti-SARS-CoV-2 antibodies and viral RNA

Sijia Yan, Khan Zara Ahmad, Antony R. Warden, Yuqing Ke, Nokuzola Maboyi, Xiao Zhi, Xianting Ding *

State Key Laboratory of Oncogenes and Related Genes, Institute for Personalized Medicine, School of Biomedical Engineering, Shanghai Jiao Tong University, Shanghai, 200030, China

ARTICLE INFO

Keywords:
SARS-CoV-2
Antibody
Viral RNA
Co-detection
Immunoassay
Pre-coated solid interface

ABSTRACT

In the field of *in vitro* diagnostics, detection of nucleic acids and proteins from biological samples is typically performed with independent platforms; however, co-detection remains a major technical challenge. Specifically, during the coronavirus disease 2019 (COVID-19) pandemic, the ability to simultaneously detect viral RNA and human antibodies would prove highly useful for efficient diagnosis and disease course management. Herein, we present a multiplex one-pot pre-coated interface proximity extension (OPIPE) assay that facilitates the simultaneous recognition of antibodies using a pre-coated antigen interface and a pair of anti-antibodies labeled with oligonucleotides. Following anti-antibody-bound nucleic acid chain extension to form templates in proximity, antibody signals can be amplified, together with that of targeted RNA, via a reverse transcription-polymerase chain reaction. Using four-color fluorescent TaqMan probes, we demonstrate the co-detection of severe acute respiratory syndrome coronavirus 2 (SARS-CoV-2)-specific antibodies and viral nucleic acids in a single biocomplex sample, including nucleocapsid protein-specific IgG and IgM, and the RNA fragments of RdRp and E genes. The serum detection limit for this platform is 100 fg/mL (0.67 fM) for the anti-SARS-CoV-2 antibody and 10 copies/μL for viral RNA. The OPIPE assay offers a practical and affordable solution for ultrasensitive co-detection of nucleic acids and antibodies from the same trace biological sample without the additional requirement of complicated equipment.

1. Introduction

The coronavirus disease 2019 (COVID-19) pandemic, caused by severe acute respiratory syndrome coronavirus 2 (SARS-CoV-2), has spread rapidly and poses a serious threat to human health (Zhou et al., 2020). In a retrospective single-center study, 249 COVID-19 cases diagnosed at Shanghai Public Health Clinical Center between January 20 and February 6, 2020, were evaluated. The median age was 51 years, 126 (50.6%) were men, and 22 (8.8%) were critically severe patients requiring intensive care unit admission. This report showed that nearly 10% of COVID-19 cases in Shanghai, China were severe and critical, highlighting the need for the development of more effective diagnostic and monitoring approaches (Chen et al., 2020).

Reverse transcription-polymerase chain reaction (RT-PCR) analysis of RNA from nasopharyngeal swabs or lung fluid is considered the gold standard to detect and confirm SARS-CoV-2 infection (Ai et al., 2020; Chan et al., 2020). Several highly sensitive and specific systems for SARS-CoV-2 RNA detection have been developed (Ma et al., 2020; Park et al., 2021). Moreover, serum testing for SARS-CoV-2 RNA can be used as an additional detection method, especially for patients with false-negative swab results as well as patients exhibiting severe infection (Zhang et al., 2020b). Additionally, conventional enzyme-linked immunosorbent assay (ELISA) for SARS-CoV-2-specific IgG and IgM can be used to detect infection and monitor recovery progress. Indeed, a combinatorial approach comprising nucleic acid and antibody quantification has been shown to increase the positive detection rate of suspected patients from 51.9% to 98.6% (Guo et al., 2020).

In addition to ELISA, alternative methods for qualitative/semi-quantitative analysis of SARS-CoV-2-specific antibodies include colloidal gold immunochromatographic analysis and lateral flow immunochromatographic analysis. Although these methods are simple, rapid, and cost-effective, they exhibit limited sensitivity and quantitative analysis capacity (Huang et al., 2020; Van Elslande et al., 2020). Currently, fluorescent microsphere immunochromatographic test strips

* Corresponding author.
E-mail address: dingxianting@sjtu.edu.cn (X. Ding).

https://doi.org/10.1016/j.bios.2021.113535
Received 21 May 2021; Received in revised form 12 July 2021; Accepted 24 July 2021
Available online 4 August 2021

for SARS-CoV-2 report the lowest limit of detection (LOD) for IgM (1 ng/mL) and IgG (30 ng/mL) antibodies, whereas microfluidic chemiluminescent ELISA can achieve an LOD of 10 pg/mL using spiked serum samples (Tan et al., 2020). According to quantitative test results, the average IgM concentrations in a weak positive sample and a strong positive sample are 20 ng/mL and 110 ng/mL, respectively, whereas the average IgG concentrations are 0.27 μg/mL and 1.88 μg/mL, respectively (Zhang et al., 2020a).

Hence, the ultrasensitive co-detection of nucleic acid and protein biomarkers in a single bio-complex sample would not only reduce the false-positive and -negative rates but would also provide insights into clinical progression. However, the current methods capable of achieving such a feat require the implementation of complex and expensive instruments as well as highly skilled technicians proficient in operating multiple platforms (Amanat et al., 2020; Stadlbauer et al., 2020).

Therefore, to address these limitations, we aimed to develop a multiplex one-pot pre-coated interface proximity extension (OPIPE) assay for the ultrasensitive co-detection of nucleic acids and proteins to reduce the burden on medical facilities, particularly in resource-limited settings. This assay is based on the recognition of antibodies using a pre-coated antigen interface and anti-antibodies labeled with oligonucleotides, which extend to double-stranded DNA templates in proximity. After adding fluorescent TaqMan probes and virus RNA template, the protein signal in the solid-phase and that of the nucleic acid in the liquid phase are simultaneously amplified via RT-PCR. In collaboration with the Shanghai Public Health Clinical Center, the sensitivity of the OPIPE assay was assessed using clinical serum samples from SARS-CoV-2-positive patients and healthy controls.

2. Material and methods

2.1. Subjects and procedures

In compliance with biosafety protocols approved by the Institutional Review Board of Shanghai Jiao Tong University, Shanghai, China (Approval No. 202003048), the performance of OPIPE assay for detecting SARS-CoV-2-specific antibody was evaluated in human serum samples. Pooled and inactive serum samples from patients with COVID-19 (age range 24–77 years) and healthy subjects (age range 28–65 years) were purchased from Elabscience Company, Ltd. (Wuhan, Hubei, China). Each participant provided written consent to participate in the study, which was approved by the regional investigational review board and performed according to the Declaration of Helsinki. The severity information for the purchased samples was provided by the phlebotomists at Elabscience during sample collection. The serum samples are from patients who were diagnosed as positive infections and later-on released from hospital after in-house treatment to ensure their serum viral RNA turned into negative. All serum samples were confirmed by RT-PCR to be free of viral nucleic acids before releasing to subsequent laboratory research use.The serum was purified by filtration through a 0.22-μm filter membrane to remove possible pathogens and impurities. The antibody concentration of both nucleocapsid protein-specific IgG and IgM (N-IgG and IgM) in thus purified serum was quantified to be 10 μg/mL based on ELISA measurement comparing with standard substance from the National Sharing Platform for Reference Materials (Beijing, China) (Fig. S1).

2.2. Oligonucleotides, reagents, and instruments

The modified oligonucleotide sequences, probes, and primers (Table S1) were sourced from Sangon Biotech Company, Ltd. (Shanghai, China). The viral sequences, primers, and probes were published by World Health Organization (https://www.who.int/docs/default-source/coronaviruse/protocol-v21.pdf?sfvrsn=a9ef618c_2). Human IgG and IgM were also purchased from Sangon Biotech. Anti-IgM polyclonal antibody (pAb) and two anti-IgG monoclonal antibodies (mAbs) with different IgG epitope targets were purchased from Kitgen Biotech (Hangzhou, Zhejiang, China). SARS-CoV-2 nucleocapsid protein and SARS-CoV-2 nucleocapsid protein-IgM and -IgG ELISA kits were purchased from Elabscience (Wuhan, Hubei, China). Sulfosuccinimidyl 4-(N-maleimidomethyl) cyclohexane-1-carboxylate (Sulfo-SMCC) and Tris-(2-carboxyethyl)-phosphine hydrochloride (TCEP·HCl) were sourced from Meilunbio (Dalian, Liaoning, China). The target sequence and primers for *in vitro* transcription of two RNA fragments of SARS-COV-2 virus and Hepatitis B virus strain 56 are provided in Tables S2 and S3. In vitro transcription, extension, and real-time fluorescent quantitative PCR were performed on a quantitative fluorescence thermal cycler (Roche LightCycler 96, Basel, Switzerland).

2.3. Generation of OPIPE probes and pre-coated antibody tubes

The technique used to produce OPIPE probes and pre-coated antibody tubes were adapted from our previous work (Yan et al., 2021). Briefly, TCEP·HCl reduced oligonucleotides were coupled with Sulfo-SMCC-activated anti-human IgG and IgM antibodies to form OPIPE probes. The recombinant SARS-CoV-2 N protein was then pre-coated on a polypropylene PCR tube to capture the specific antibody.

2.4. OPIPE assay detection

Positive and negative serum were diluted with a proportional concentration gradient. All details pertaining to the incubation, extension, and washing processes are described in our previous reports (Yan et al., 2021). Prior to performing RT-PCR, the SARS-CoV-2 RNA fragments, PrimeDirect™ Probe RT-qPCR Mix (Takara, Japan), RNase-free H_2O, and four sets of probe primers were simultaneously added to the reaction tubes. The reaction system is shown in Table S4. All PCR reactions were performed in a 25 μL reaction volume on a LightCycler 96 (Roche, Switzerland) under the manufacturer's recommended fast cycling conditions for 40 cycles. The instrument was adjusted to simultaneously record signals from all four channels.

2.5. Statistical analysis

For each data point, the raw $-\Delta C_t$ value was normalized by subtracting the C_t value for the extension control reaction from that of the corresponding sample, thereby correcting for technical variation. All linear regression analyses and curve fitting were performed using Origin 9.0. Two-tailed Student's *t*-tests were performed using Microsoft Excel 2016 to calculate P-values. A two-sided P-value < 0.05 was considered statistically significant.The relative standard deviations (RSD) were also calculated for repilcated tests.

3. Results and discussion

3.1. Oligonucleotide design, construction, and purification for the OPIPE assay

As a proof of concept, we used OPIPE to simultaneously detect two SARS-CoV-2 RNA fragments, which encode from Envelope (E) and RNA-dependent RNA polymerase (RdRP) gene of SARS-Cov-2 virus and two human antibodies (N-IgM and N-IgG). These dual-RNA assays help to reduce false-negative results caused by the degradation of partial fragments and amplification inhibition (Erhu et al., 2020; Kim et al., 2020; Trémeaux et al., 2020). Additionally, the dual-antibody assay can provide information regarding the stage of disease and the immune status of the patient. The pipeline for co-detection is illustrated in Fig. 1, while the details of the OPIPE assay are presented in Fig. 2A. As shown in Fig. 2B, co-detection of viral nucleic acids and specific antibodies can be used to evaluate the clinical course of patients with COVID-19.

The probe oligonucleotide sequences in the OPIPE assay were

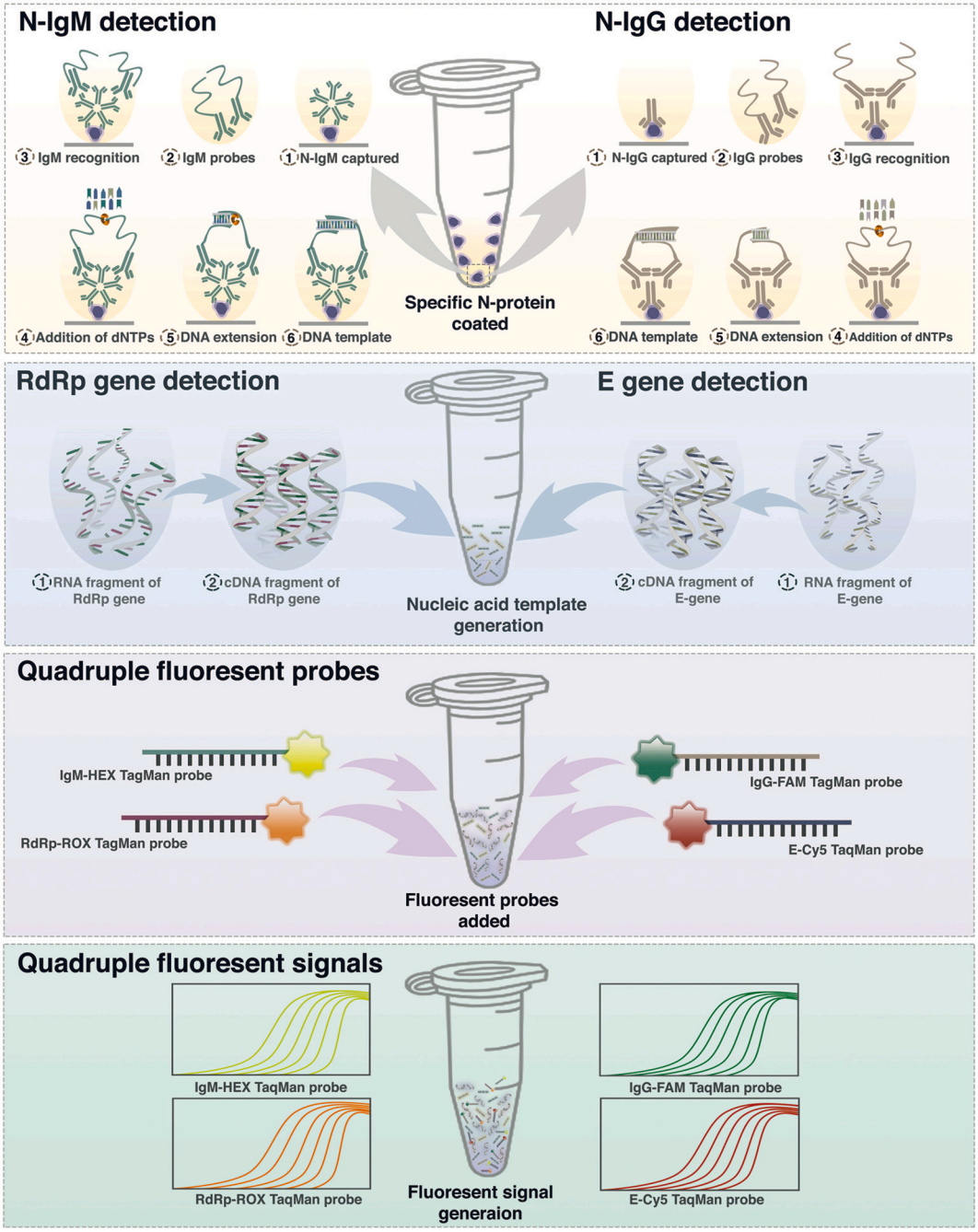

Fig. 1. Schematic of OPIPE assay, a one-pot reaction cascade for co-detection of N protein-specific antibodies and viral nucleic acids in one bio-complex sample.

designed to contain the unique binding sites for the primers and TaqMan probes. For the 3′-linked probe, we designed a 57-mer oligonucleotide that included 28-bases corresponding to the 5′-linked probe and unique binding sites for specific primers used in qPCR. Primers were generated using Primer-BLAST (https://www.ncbi.nlm.nih.gov/tools/primer-blast/). Considering that the TaqMan probe was used in this experiment, we optimized the design scheme of the probe based on the following logic. The 5′-end of the TaqMan probe must be in close proximity with the 3′-end of the forward primer; the length of the probe should be approximately 25 bp, its GC content should be 50–70%, and guanine should be avoided as the first base at the 5′-end. Importantly, alignment of the sequences for the synthetic oligonucleotide, human genome, and other coronavirus genomes revealed no homology. Oligonucleotide sequences, primers, and TaqMan probes for the detection of N-IgM and N-IgG are shown in Fig. 2C and Table S1. The probes used in the OPIPE assay were generated through Sulfo-SMCC-driven conjugation of 5′-thiol-modified oligonucleotides to a pair of monoclonal mouse anti-human IgG antibodies (anti-IgG mAb) or polyclonal rabbit anti-human IgM antibodies (anti-IgM pAb) following amino activation. Successful probe synthesis was confirmed via nucleic acid and protein detection using sodium dodecyl sulfate polyacrylamide gel electrophoresis, followed by staining with GelRed and Coomassie Brilliant Blue, respectively (Fig. 2D and E). Subsequently, the probes were purified using centrifugal filtration membranes with a 100-kDa cut-off and stored at −20 °C until use.

3.1.1. *Detection of IgG and IgM at the femtomolar level using OPIPE assay*

To optimize the assay pipeline, polypropylene tubes used for conventional PCR were treated with an 8% glutaraldehyde solution and precoated with either mouse anti-human IgG or rabbit anti-human IgM (Yin

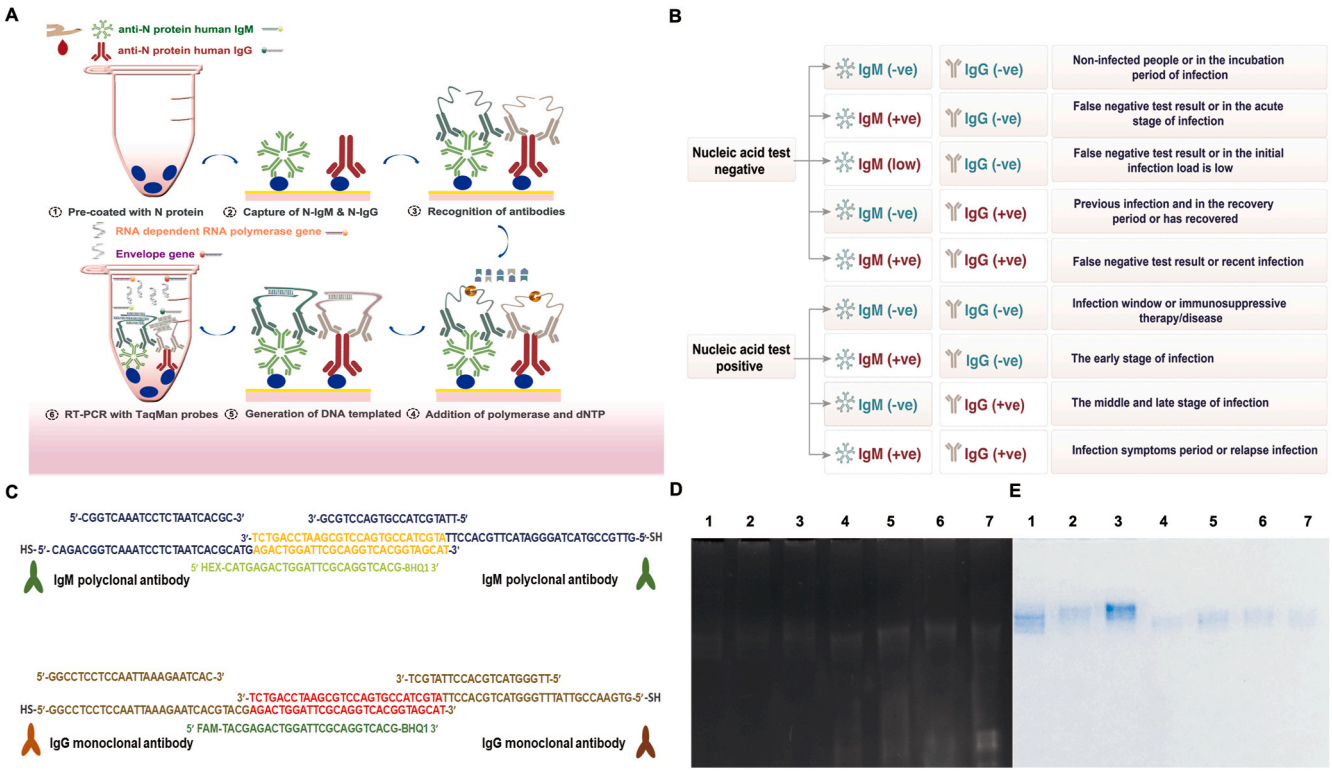

Fig. 2. The co-analytical determination of nucleic acid and antibody detection to evaluate SARS-CoV-2 infection and clinical course. (A) Details of one-pot pre-coated interface proximity extension assay. (B)Table of co-analytical test results and clinical diagnoses. (C)Oligonucleotides and primers are designed for the detection of IgM and IgG. (D) and (E) Representative gel images of antibody and probe components. Lane information: (1) IgM polyclonal antibody, (2) IgG monoclonal antibody 1, (3) IgG monoclonal antibody 2, (4) IgM probe 1, (5) IgM probe 2, (6) IgG probe 1, (7) IgG probe 2.

et al., 2013). The tubes were then incubated with 10% and 100% human serum spiked with a 100-fold dilution series of IgG or IgM at concentrations ranging from 100 fg/mL to 10 μg/mL. After washing away unbound substances that were not captured by the tube-coated anti-antibody, the probes were incubated with target IgG or IgM. When tube-coated anti-antibodies and probes simultaneously recognized IgG or IgM, the oligonucleotides of the probes in close proximity were subjected to an extension reaction with T4 polymerase. RT-PCR was then performed following addition of the TaqMan probes and primers to the tubes; signals were subsequently recorded. The estimated LOD in 10% serum was 100 fg/mL, and the correlation coefficients (R^2) calculated by regression of measured $-\Delta C_t$ values (C_t value of sample minus that of the control) on logarithmic concentrations of IgG or IgM were 0.990 and 0.994, respectively, in the linear range between 100 fg/mL and 10 μg/mL. Moreover, although the $-\Delta C_t$ values in 100% serum are lower than in 10% serum, the estimated LOD and linear fit are almost the same (Fig. S2).

3.2. Ultra-high sensitivity of OPIPE assay in donor serum

After confirming the effectiveness of the probe for N-IgG and -IgM, the polypropylene tubes were immobilized with SARS-CoV-2-specific N protein following the aforementioned protocol. To improve the efficiency of capturing specific antibodies in COVID-19-positive donor serum, we optimized the N protein concentration at the solid–liquid phase interface in the tubes. Different concentrations of N protein (2, 4, and 8 μg/mL) were added to the glutaraldehyde-treated tubes at 4 °C overnight. After washing, the tube interface was blocked with 1% BSA and washed three times.

COVID-19 positive or negative donor serum samples used in this study were inactivated and purified. The concentration of antibodies in the undiluted positive donor serum was 10 μg/mL. Diluted COVID-19 positive serum containing 10 pg/mL and 1 ng/mL N-IgG were incubated in pre-coated tubes with different concentrations of antibodies. OPIPE probes were subsequently added, extended, and amplified according to the steps in the section 2.1 describing the detection of IgG and IgM by the OPIPE assay. Analysis of qPCR results revealed significantly higher −ΔCt values in tubes pre-coated with 8 μg/mL N protein compared to those coated with a lower concentration (P-value<0.05). Notably, for a diluted serum containing 10 pg/mL N-IgG, the mean $-\Delta C_t$ values increased from 0.35 (in 2 μg/mL N protein pre-coated tubes) to 1.12 (in 8 μg/mL N protein pre-coated tubes), corresponding to a more than 3-fold increase (Fig. S3). Therefore, 8 μg/mL was used as the coating concentration for the tube interface in all subsequent experiments.

Next, COVID-19 positive or negative sera were subjected to 100-fold serial dilution and incubated in the 8 μg/mL N protein pre-coated tubes. Probe incubation and extension were performed as described above. The N-IgG and -IgM signals were obtained after PCR amplification using primers and specific TaqMan probes carrying the fluorescent reporters FAM and HEX, respectively (Table S1). The estimated LOD in COVID-19 positive serum was 100 fg/mL, and the R^2 of the measured $-\Delta C_t$ value using logarithmic concentrations of N-IgG or -IgM were 0.995 and 0.991, respectively, in the linear range between 10 pg/mL and 10 μg/mL. The RSD was 2.99% and 4.22% for IgG and IgM at the highest concentration (10 μg/mL).In the linear range, the RSD for the detection of IgM and IgG in positive serum was 10.76% ± 3.85% and 9.82% ± 4.17%, respectively. Due to the relatively weak signal, the RSD for the lowest concentrations was around 15%. Significant differences ($P < 0.05$) were observed in −ΔCt values between the positive and negative serum samples at each dilution, indicating that definitive diagnosis could be made using serum samples diluted up to 10,000,000-times, and clinical samples could be adequately preserved (Fig. 3A–F). We also compared the abilities of the OPIPE assay to detect N-IgM and N-IgG

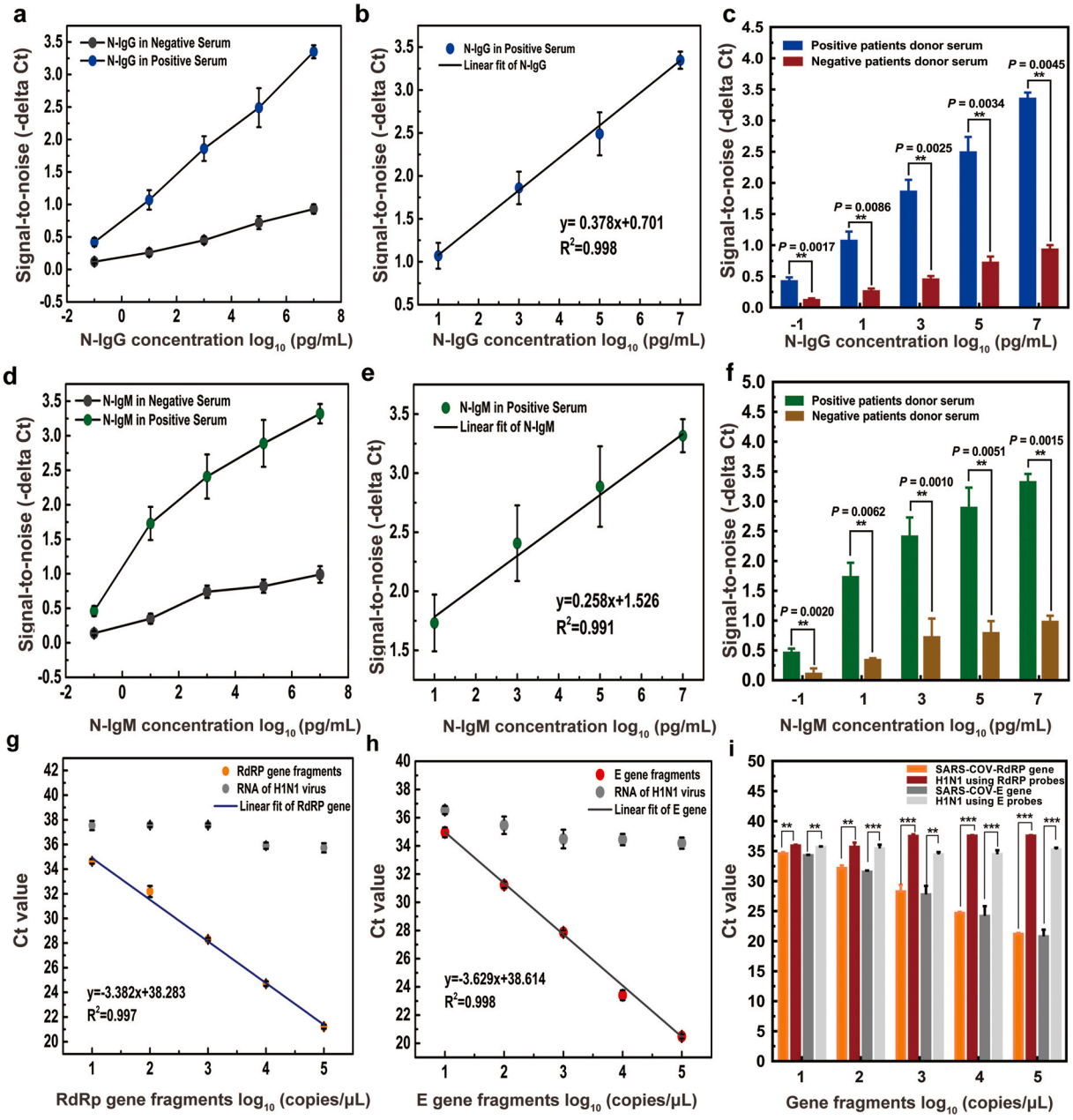

Fig. 3. OPIPE assays were performed for human IgG and IgM in 10% COVID-19 positive donor serum and negative serum. (A–F) The complete standard curves (100 fg to 10 μg mL) and linear regression analysis (10 pg–10 μg mL) for a series dilution of N-IgG and N-IgM. Significant differences in -ΔCt values between positive and negative serum samples at each dilution concentration (100 fg to 10 μg/mL) of N-IgG and N-IgM. A two-sided P-value < of 0.05 was considered statistically significant. (G–I) Linear fitted lines or bars show the C_t values obtained by PCR amplification of the RdRP and E gene fragments with a non-complementary sequence of the H1N1 virus and diluted to different concentrations (10 to 10^5 copies/μL) in parallel tubes. The C_t values of a non-complementary sequence of H1N1 virus is significantly higher than that of the RdRP and E gene fragments at all concentration. All data are presented as the mean ± standard deviation. Each experiment had five technical replicates.

with standard ELISA (Table S5). Furthermore, we did experiments with narrower dilutions (10-fold) of serum for both N-IgM and N-IgG (Fig. S4). Our results indicate that the linearity is not significantly shifted between different dilution factors. To verify the repeatability of the method, we also performed the experiments at different times (Table S6).

3.3. Co-detection of SARS-CoV-2 RNA fragments in parallel tubes

Due to the strict prevention requirements of COVID-19 in China, we could not obtain viral RNA or serum containing RNA from patients. As an alternative, we added *in vitro* synthesized RNA fragments to the positive donor serum. To co-detect nucleic acids and specific antibodies in the same bio-complex-containing sample, we added 10^5 copies RNA transcripts of the E and RdRP genes to the donor serum and then diluted them in 10-fold series dilution. A commercially available one-step RT-qPCR mix included in the same setup was used for antibody detection. The primer and probe with ROX and Cy5 fluorescent reporters are listed in Table S1. Primers and probes were specific to the SARS-CoV-2 genome sequence and were cross-validated to ensure no homology in sequence alignment with human SARS-CoV and bat-SARS-related CoV genomes (Fig. S5). The PCR amplification signal of RNA is exhibited with C_t values, which are inversely proportional to the concentration of the nucleic acid fragments. The C_t values of a non-complementary sequence

of H1N1 virus is significantly higher than that of the RdRP and E gene fragments at all concentration(Fig. 3G–I). Results from three different time points are presented in Table S7.

3.4. OPIPE enables ultrasensitive RNA and antibody co-detection in one pot

The above experiments were carried out in parallel tubes using the same equipment. To achieve true co-detection in one pot,10^5 copies of RNA transcripts of the E and RdRP genes were spiked into the positive serum. Then we added the positive serum in 10-fold series dilution in the same tube before RT-PCR. All four sets of TaqMan probes and primers required for the one-pot reaction were then added and co-detected using the one-step RT-qPCR Probe Kit. The reaction conditions used for the simultaneous one-pot co-detection of SARS-CoV-2 RNA as well as minor adjustments required for patient antibodies based on separate assays, are detailed in Table S4.

Our results showed that the signal generated by the one-pot reaction differed slightly from those obtained for the individual separate reactions; however, the sensitivity was not significantly affected. Moreover, compared with the results of the separate detection methods, IgG and IgM showed a slightly lower $-\Delta Ct$ value at a relatively higher RNA concentration, and a higher $-\Delta Ct$ value at lower RNA concentrations. Additionally, the estimated LOD for N-IgG and -IgM in 10% COVID-19-positive serum was 100 fg/mL, with R^2 values (of measured Ct values on a logarithmic scale) of 0.995 and 0.991, respectively, in the linear range

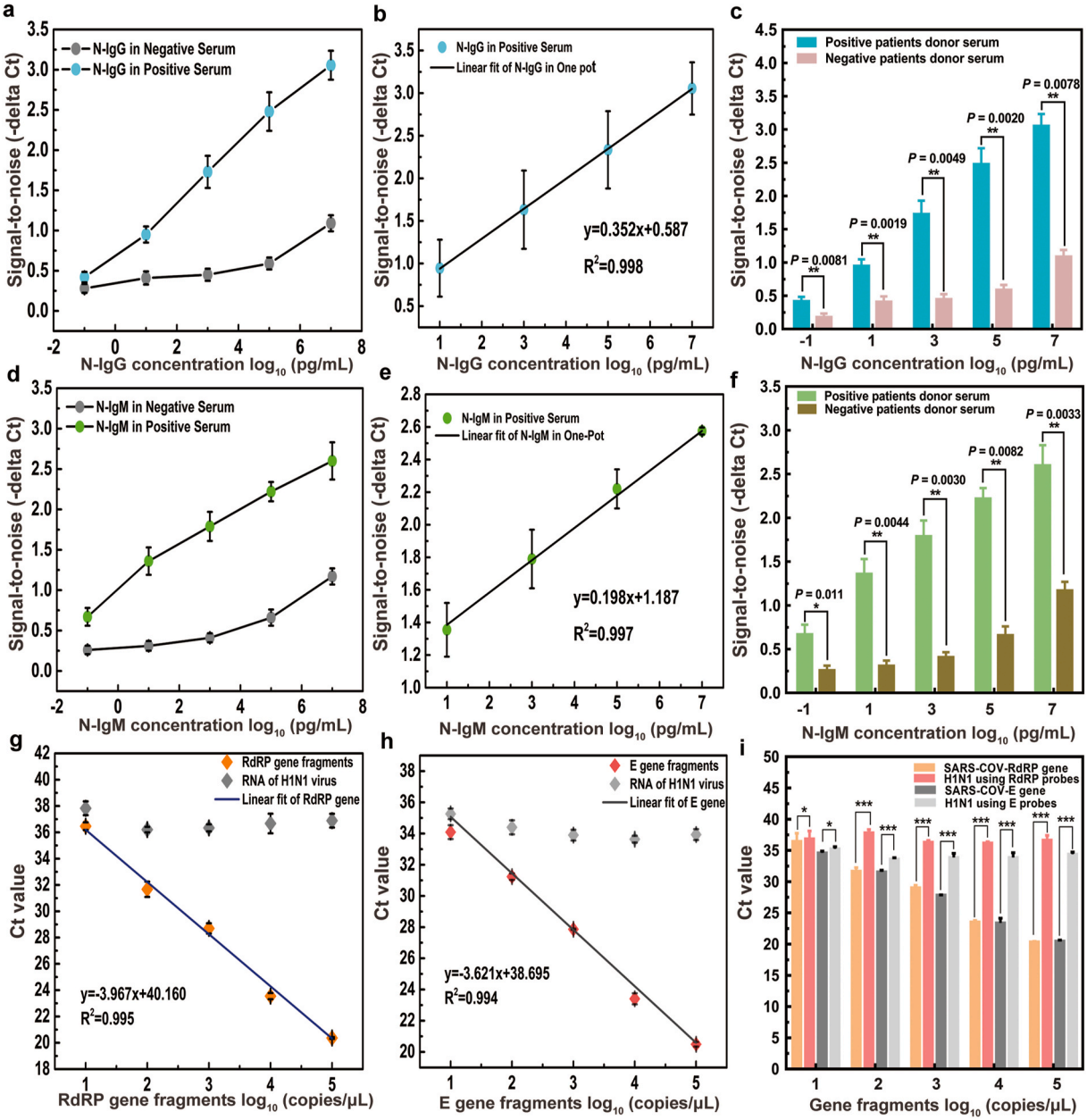

Fig. 4. Antibody and nucleic acid co-detection in 10% COVID-19 positive and negative donor serum through the one-pot assay. (**A-F**) The complete standard curves (100 fg to 10 μg/mL) and linear regression analysis (10 pg–10 μg/mL) for solutions of N-IgG and N-IgM. C and F, There were significant differences in $-\Delta C_t$ values between positive and negative serum samples at each dilution concentration of N-IgG and N-IgM. (**G-I**) Linear fitted lines or bars show the C_t values obtained by PCR amplification of the RdRP and E gene fragments with a non-complementary sequence of the H1N1 virus and diluted to different concentrations in one-pot (10 to 10^5 copies/μL). The C_t values of RNA fragments of H1N1 virus is significantly higher than that of the RdRP and E gene fragments at all concentration. All data are presented as the mean ± standard deviation. Each experiment had five technical replicates.

between 10 pg and 10 μg/mL. Within the linear range, the RSD of OPIPE assay for IgG and IgM detection in positive serum was 9.41 ± 2.47 and 9.20 ± 2.95, respectively. Significant differences ($P < 0.05$) were observed in the −ΔCt values between positive and negative serum samples at each dilution (Fig. 4A–F). The nucleic acid results showed no change in sensitivity down to 10 copies/μL, with a robust linear relationship observed between RdRP ($R^2 = 0.995$) and E gene detection ($R^2 = 0.998$). In the one-pot OPIPE assay, the C_t values of a non-complementary sequence is significantly higher than that of the RdRP and E gene fragments at all concentration Fig. 4G-I).

3.5. Low cross-reactivity of the OPIPE assay

In addition to sensitivity, we further examined the cross-reactivity of the OPIPE assay. Cross-reactivity refers to an extraneous signal caused by the binding of a non-target protein similar to the expected target protein. In this experiment, we added non-SARS-CoV N protein-specific human IgG and IgM to 10% human serum diluted with PBS. In a 100-fold dilution series of IgG or IgM at concentrations ranging from 100 fg/mL to 10 μg/mL, the OPIPE assay showed no significant cross-reactive signals. The −ΔCt values at the highest concentration of 100 ng/mL were still lower than at the lowest concentration of 100 fg/mL in COVID-19-positive donor serum (Fig. 5A). Moreover, we evaluated the cross-reactivity of TaqMan probe and primer sets by adding two interfering RNAs, namely RNA fragments of hepatitis B virus (HBV) and the complete RNA of influenza A virus (H1N1), to the SARS-CoV-2 RdRP and E gene fragments. Addition of the two interfering RNAs had no significant effect on the detection signal of RdRP and E genes. As a negative control, the amplification of two non-SARS-CoV-2 sequences, HBV and H1N1 viral fragments, exhibited no significant difference compared with the background containing no viral fragment (Fig. 5B).

We compare the LOD of our OPIPE with the existing commercial ELISA assay (approved for emergency-use-administration by Food and Drug Administration), the LOD of which ranges 1.6–13,500 ng/mL by using real patient samples. Although both OPIPE and ELISA take about 2 h, OPIPE reduces the detection limit from pM to fM concentration range. Moreover, the OPIPE assay exhibited enhanced sensitivity for antibody detection compared to previously reported methods (Table 1) and two protein signal amplification strategies, the solid-phase proximity ligation assay (LOD: 0.01 pM) and homogeneous proximity extension assay (LOD:0.05 pM) (Jiang et al., 2014; Nong et al., 2013). The OPIPE assay also facilitates the detection of specific antibodies and nucleic acids in ultra-low volume blood samples, including those obtained via finger prick, with a throughput of up to 96 assays using only PCR instrument, thus satisfying the requirements for simultaneous detection of specific antibodies and nucleic acids from patients and demonstrating its application for healthcare facilities within resource-limited regions. For practical clinical application, we were also able to convert our measurement results into N-IgG and IgM concentration using the standard curve in Figs. 3 and 4.

Table 1
The comparison between the OPIPE assay and other methods of detection of SARS-CoV-2 specific antibody.

The detection method of SARS-CoV-2 specific antibody (IgG or IgM)	Orders of magnitude	LOD[a)]	Ref.
Fluorescent microsphere immune chromatographic test strips	4	1 ng/mL for IgM and 30 ng/mL for IgG	Zhang et al. (2020a)
Microfluidic chemiluminescent ELISA technology	5	10 pg/mL	Tan et al. (2020).
Nanostructured plasmonic gold (pGOLD) assay	4	1.6 ng/mL	Liu et al. (2020)
Electrochemical impedance-based sensing (EIS) assay	3	0.1 μg/mL	Rashed et al. (2021)
Opto-microfluidic sensing platform with gold nanospikes	3	0.08 ng/mL	Funari et al. (2020)
Laser-engraved graphene immunosensors	4	500 pg/mL	Torrente-Rodríguez et al. (2020)
Microfluidic nanoimmunoassay	5	1 nM	Swank et al. (2021)
One-pot PRe-coated antibOdy Proximity Extension (OPIPE) assay	5	100 fg/mL	This method

[a] LOD:limit of detection.

4. Conclusion

Certain limitations were noted in this study. For instance, the OPIPE protocol must be conducted in a biosafety laboratory when handling infectious pathogens since the washing steps in the current protocol require uncapping operations. Furthermore, the incubation and extension of OPIPE probes as well as the addition of RNA template and primers, should be performed in separate areas to maximally avoid cross-contamination. Nevertheless, we report that the OPIPE assay, a one-pot diagnostic procedure, can simultaneously detect nucleic acids and proteins in the same trace clinical sample. This strategy significantly

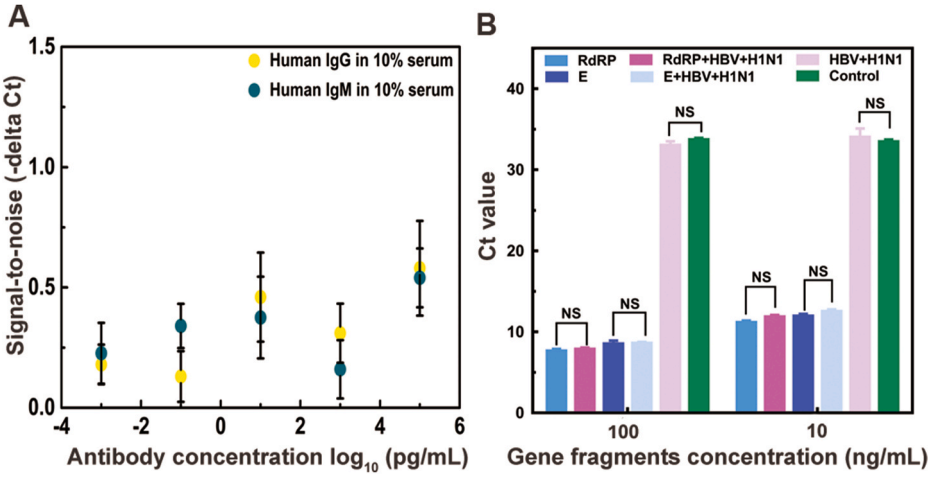

Fig. 5. Cross-reactivity of the OPIPE assay with non-SARS-CoV-2 specific nucleic acids and antibodies. (A) The signal change from 100 fg to 10 μg/mL for a series solution of non-SARS-CoV nucleocapsid protein-specific human IgG and IgM standards in 10% serum. (B) At two different concentrations, 100 and 10 ng/mL, there was no significant difference between the amplification signal of RdRP gene fragment alone (blue) or that with two non-SARS-COV-2 RNA fragment, fragment of HBV and H1N1(purplish red). Similarly, there was no significant difference between the amplification signals (dark blue) of the E gene alone or that with two non-SARS-COV-2 RNA fragments, fragments of HBV and H1N1 (light blue). Comparison of the amplification signal of the two non-SARS-COV-2 RNA segments for HBV and H1N1(pink) alone with the background containing no viral segments (green) revealed no significant differences. (For interpretation of the references to color in this figure legend, the reader is referred to the Web version of this article.)

enhances the specific binding of the target protein with immunoglobulins present in patient serum. Moreover, our platform possesses a high sensitivity of 100 fg/mL (0.67 fM) in serum, representing a minimum 15-fold enhancement over that of solid-phase proximity ligation assays (0.01 pM). Moreover, the OPIPE nucleic acid results exhibited high sensitivity (10 copies/mL). Importantly, the OPIPE assay has an ultrasensitive detection limit and does not require any additional sophisticated instrumentation, making it accessible to clinical settings in resource-limited regions. By changing the antibodies and oligonucleotides, this platform can be readily tailored for the early diagnosis of other diseases and basic research in single cells.

CRediT authorship contribution statement

Sijia Yan: Conceptualization, Data curation, Formal analysis, Investigation, Writing – original draft, Writing – review & editing. **Khan Zara Ahmad:** Formal analysis, Methodology, Graph making. **Antony R. Warden:** Investigation, Resources. **Yuqing Ke:** Data curation, Formal analysis, Investigation. **Nokuzola Maboyi:** Formal analysis, Investigation. **Xiao Zhi:** Formal analysis. **Xianting Ding:** Writing – original draft, Writing – review & editing, Project administration, Funding acquisition.

Declaration of competing interest

The authors declare that they have no competing financial interests or personal relationships that could have influenced the work reported in this paper.

Acknowledgements

The authors thank the staff at AEMD SJTU for their support.

Appendix A. Supplementary data

Supplementary data to this article can be found online at https://doi.org/10.1016/j.bios.2021.113535.

Funding

We gratefully thank the financial support from NSFC Projects (22077079, 81871448), Shanghai Sailing Program [19YF1446900]; Shanghai Municipal Science and Technology Project (2017SHZDZX01, and 18430760500), Shanghai Agriculture Applied Technology Development Program Project (G20180101), Shanghai Municipal Education Commission Project (ZXWF082101), Ministry of Science and Technology of China Project (2017ZX10203205-006-002), Shanghai Jiao Tong University Projects (YG2021ZD19, Agri-X20200101, SL2020MS026, 19X190020154, ZH2018ZDA01, YG2016QN24, YG2016MS60, 2020 SJTU-HUJI, SD0820016), Shanghai Municipal Health Commission Project (2019CXJQ03), Shanghai Clinical Medical Research Center Project 19MC1910800, National Innovation Special Zone Project. Thanks to AEMD SJTU for the support. The funding source played no role in study design; in the collection, analysis, and interpretation of data; in the writing of the report; or the decision to submit the article for publication.

References

Ai, T., Yang, Z., Hou, H., Zhan, C., Chen, C., Lv, W., Tao, Q., Sun, Z., Xia, L., 2020. Radiology 296 (2), E32–E40.
Amanat, F., Stadlbauer, D., Strohmeier, S., Nguyen, T.H.O., Chromikova, V., McMahon, M., Jiang, K., Arunkumar, G.A., Jurczyszak, D., Polanco, J., Bermudez-Gonzalez, M., Kleiner, G., Aydillo, T., Miorin, L., Fierer, D.S., Lugo, L.A., Kojic, E.M., Stoever, J., Liu, S.T.H., Cunningham-Rundles, C., Felgner, P.L., Moran, T., García-Sastre, A., Caplivski, D., Cheng, A.C., Kedzierska, K., Vapalahti, O., Hepojoki, J.M., Simon, V., Krammer, F., 2020. Nat. Med. 26 (7), 1033–1036.
Chan, J.F.-W., Yip, C.C.-Y., To, K.K.-W., Tang, T.H.-C., Wong, S.C.-Y., Leung, K.-H., Fung, A.Y.-F., Ng, A.C.-K., Zou, Z., Tsoi, H.-W., Choi, G.K.-Y., Tam, A.R., Cheng, V.C.-C., Chan, K.-H., Tsang, O.T.-Y., Yuen, K.-Y., 2020. J. Clin. Microbiol. 58 (5) e00310-00320.
Chen, J., Qi, T., Liu, L., Ling, Y., Qian, Z., Li, T., Li, F., Xu, Q., Zhang, Y., Xu, S., Song, Z., Zeng, Y., Shen, Y., Shi, Y., Zhu, T., Lu, H., 2020. J. Infect. 80 (5), e1–e6.
Erhu, X., Jiang, L., Tian, T., Hu, M., Yue, H., Huang, M., Lin, W., Jiang, Y., Zhu, D., Zhou, X., 2020. Angew. Chem. Int. Ed. 60 (10), 5307–5315.
Funari, R., Chu, K.-Y., Shen, A.Q., 2020. Biosens. Bioelectron. 169, 112578.
Guo, L., Ren, L., Yang, S., Xiao, M., Chang, D., Yang, F., Dela Cruz, C.S., Wang, Y., Wu, C., Xiao, Y., Zhang, L., Han, L., Dang, S., Xu, Y., Yang, Q.-W., Xu, S.-Y., Zhu, H.-D., Xu, Y.-C., Jin, Q., Sharma, L., Wang, L., Wang, J., 2020. Clin. Infect. Dis. 71 (15), 778–785.
Huang, C., Wen, T., Shi, F.-J., Zeng, X.-Y., Jiao, Y.-J., 2020. ACS Omega 5 (21), 12550–12556.
Jiang, X., Zhou, L., Cheng, J., Zhang, H., Wang, H., Chen, Z., Shi, F., Zhu, C., 2014. Anal. Chim. Acta 841, 17–23.
Kim, D., Lee, J.-Y., Yang, J.-S., Kim, J.W., Kim, V.N., Chang, H., 2020. Cell 181 (4), 914-921.e910.
Liu, T., Hsiung, J., Zhao, S., Kost, J., Sreedhar, D., Hanson, C.V., Olson, K., Keare, D., Chang, S.T., Bliden, K.P., Gurbel, P.A., Tantry, U.S., Roche, J., Press, C., Boggs, J., Rodriguez-Soto, J.P., Montoya, J.G., Tang, M., Dai, H., 2020. Nat. Biomed. Eng. 4 (12), 1188–1196.
Ma, P., Meng, Q., Sun, B., Zhao, B., Dang, L., Zhong, M., Liu, S., Xu, H., Mei, H., Liu, J., Chi, T., Yang, G., Liu, M., Huang, X., Wang, X., 2020. Adv. Sci. 7 (20), 2001300.
Nong, R.Y., Wu, D., Yan, J., Hammond, M., Gu, G.J., Kamali-Moghaddam, M., Landegren, U., Darmanis, S., 2013. Nat. Protoc. 8 (6), 1234–1248.
Park, J.S., Hsieh, K., Chen, L., Kaushik, A., Trick, A.Y., Wang, T.-H., 2021. Adv. Sci. 8 (5), 2003564.
Rashed, M.Z., Kopechek, J.A., Priddy, M.C., Hamorsky, K.T., Palmer, K.E., Mittal, N., Valdez, J., Flynn, J., Williams, S.J., 2021. Biosens. Bioelectron. 171, 112709.
Stadlbauer, D., Amanat, F., Chromikova, V., Jiang, K., Strohmeier, S., Arunkumar, G.A., Tan, J., Bhavsar, D., Capuano, C., Kirkpatrick, E., Meade, P., Brito, R.N., Teo, C., McMahon, M., Simon, V., Krammer, F., 2020. Curr. Protoc.Microbiol. 57 (1), e100.
Swank, Z., Michielin, G., Yip, H.M., Cohen, P., Andrey, D.O., Vuilleumier, N., Kaiser, L., Eckerle, I., Meyer, B., Maerkl, S.J., 2021. P. Natl. Acad. Sci. Usa 118 (18), e2025289118.
Tan, X., Krel, M., Dolgov, E., Park, S., Li, X., Wu, W., Sun, Y.-L., Zhang, J., Khaing Oo, M. K., Perlin, D.S., Fan, X., 2020. Biosens. Bioelectron. 169, 112572.
Torrente-Rodríguez, R.M., Lukas, H., Tu, J., Min, J., Yang, Y., Xu, C., Rossiter, H.B., Gao, W., 2020. Matter 3 (6), 1981–1998.
Trémeaux, P., Lhomme, S., Abravanel, F., Raymond, S., Mengelle, C., Mansuy, J.-M., Izopet, J., 2020. J. Clin. Virol. 129, 104541.
Van Elslande, J., Houben, E., Depypere, M., Brackenier, A., Desmet, S., André, E., Van Ranst, M., Lagrou, K., Vermeersch, P., 2020. Clin. Microbiol. Infect. 26 (8), 1082–1087.
Yan, S., Ahmad, K.Z., Li, S., Warden, A.R., Su, J., Zhang, Y., Yu, Y., Zhi, X., Ding, X., 2021. Biosens. Bioelectron. 183, 113211.
Yin, H., Zhu, Y., Xu, L., Kuang, H., Wang, L., Xu, C., 2013. Biosens. Bioelectron. 42, 51–55.
Zhang, C., Zhou, L., Liu, H., Zhang, S., Tian, Y., Huo, J., Li, F., Zhang, Y., Wei, B., Xu, D., Hu, J., Wang, J., Cheng, Y., Shi, W., Xu, X., Zhou, J., Sang, P., Tan, X., Wang, W., Zhang, M., Wang, B., Zhou, Y., Zhang, K., He, K., 2020a. Emerg. Microb. Infect. 9 (1), 2020–2029.
Zhang, W., Du, R.-H., Li, B., Zheng, X.-S., Yang, X.-L., Hu, B., Wang, Y.-Y., Xiao, G.-F., Yan, B., Shi, Z.-L., Zhou, P., 2020b. Emerg. Microb. Infect. 9 (1), 386–389.
Zhou, P., Yang, X.-L., Wang, X.-G., Hu, B., Zhang, L., Zhang, W., Si, H.-R., Zhu, Y., Li, B., Huang, C.-L., Chen, H.-D., Chen, J., Luo, Y., Guo, H., Jiang, R.-D., Liu, M.-Q., Chen, Y., Shen, X.-R., Wang, X., Zheng, X.-S., Zhao, K., Chen, Q.-J., Deng, F., Liu, L.-L., Yan, B., Zhan, F.-X., Wang, Y.-Y., Xiao, G.-F., Shi, Z.-L., 2020. Nature 579 (7798), 270–273.